SEMARAK ILMU PUBLISHING

Journal of Advanced Research in Fluid Mechanics and Thermal Sciences

Journal homepage:
https://semarakilmu.com.my/journals/index.php/fluid_mechanics_thermal_sciences/index
ISSN: 2289-7879

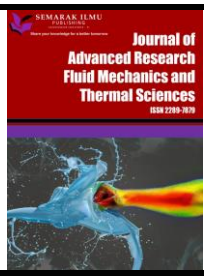

The High-Performance Polymer Electrolytes Based on Agarose–$Mg(ClO_4)_2$ for Application in Electrochemical Energy Storage Devices

Nurul Izzati Ali[1], Siti Zafirah Zainal Abidin[1,2,*], Siti Rohana Majid[3]

[1] Faculty of Applied Sciences, Universiti Teknologi MARA, 40450 Shah Alam, Selangor, Malaysia
[2] Ionic Materials and Devices (iMADE) Research Laboratory, Institute of Science, Universiti Teknologi MARA, 40450 Shah Alam, Selangor, Malaysia
[3] Centre for Ionics University of Malaya, Department of Physics, Faculty of Science, University of Malaya, 50603, Kuala Lumpur, Malaysia

ARTICLE INFO

Article history:
Received 26 December 2023
Received in revised form 11 May 2024
Accepted 22 May 2024
Available online 15 June 2024

Keywords:
Agarose; magnesium perchlorate; polymer electrolyte; electrical; electrochemical

ABSTRACT

Electrochemical energy storage devices (EES) such as batteries and supercapacitors depend significantly on electrolytes, which have properties that significantly impact their energy capacity, rate performance, cyclability, and safety. Agarose–$Mg(ClO_4)_2$–based polymer electrolyte was prepared using the solution casting method by incorporating various amounts of $Mg(ClO_4)_2$ from 0 – 35 wt%. The presence of $Mg(ClO_4)_2$ as the dopant in agarose-matrix enhanced the ionic conductivity of the system from 1.796×10^{-8} S·cm^{-1} to 6.247×10^{-4} S·cm^{-1} in the composition of 30 wt% $Mg(ClO_4)_2$ due to the production of free ions. This system obeys the Arrhenius rule as it records the conductivity increment when temperature increases. This increment shows the amorphous nature of electrolytes, which XRD analyses by determining the crystallite size and degree of crystallinity of agarose–$Mg(ClO_4)_2$ polymer electrolyte. High ionic conductivity at room temperature has increased attention to this polymer electrolyte based on agarose–$Mg(ClO_4)_2$.

1. Introduction

A biopolymer is a polymer produced by living organisms, decomposed naturally in the environment, and has been studied rapidly for applying energy storage devices as electrolytes [1]. Biopolymers, also called natural polymers, can be used as host materials in creating polymer electrolytes because they are inexpensive, plentiful in nature, non-toxic, safe, and biodegradable. Polymer electrolytes are materials that can conduct ions while being solid, and they have been extensively studied for use in electrochemical devices such as batteries, supercapacitors, and fuel cells. One of the main challenges in developing polymer electrolytes is achieving a balance between ion conductivity and mechanical strength. Polysaccharide biopolymers have been investigated as host polymers that can provide both properties due to their ability to form a promising film [2,3]. Because of their high molecular weight, polysaccharides can form a dense film through strong

* *Corresponding author.*
E-mail address: szafirah@uitm.edu.my

https://doi.org/10.37934/arfmts.118.1.6585

intermolecular interactions, enabling the movement of ions, which is essential for a polymer electrolyte's functionality. Additionally, polysaccharides have a high hydration level, which can facilitate ion solvation and movement.

In this study, biopolymer agarose, one of the natural polysaccharides found in seaweed, is chosen as the host polymer matrix for ionic conduction. According to Yang *et al.,* [4], agarose (d-galactose and 3,6-anhydro-1-galactopyranose) is one of the polysaccharides rich with a hydroxyl group in their molecule structure. This results in a cross-linking network with other components in polymer electrolyte and proves that agarose is an effective polymer matrix as it can promote the transportation of ions [5,6]. Moreover, polysaccharides also reserve much lower crystallinity and higher ionic conductivity than non-polysaccharide polymers such as Polyethylene Oxide (PEO), which recorded about 10^{-8}–10^{-7} S·cm^{-1} [3,6]. In addition, using polysaccharides as a polymer matrix may produce an electrolyte with good thermal and chemical stability [4]. Agarose seems to be a perfect candidate for this research as it can form a stable gel and thick film without affecting ionic conductivity [5]. This proves that agarose-based polymer electrolytes possess mechanical strength and conductivity that is liquid-like [7]. These elucidations were confirmed as Ali *et al.,* [8] recorded an exhibition of 1.48×10^{-5} S·cm^{-1} value in ionic conductivity in their study, where agarose was used as a polymer matrix. Another research related to agarose-based biopolymer electrolytes was done by Singh and the team (2017), which reported the production of a high ionic conductivity value of about 7.41×10^{-3} S·cm^{-1} with the addition of 1-ethyl-3-methylimidazolium dicyanamide (EMImDCA) in the composition.

Salt is an essential component to be implemented in preparing polymer electrolytes as it consists of ions required for the conduction process in the polymer matrix. The presence of salt can reduce the degree of crystallinity, enhance the ionic conductivity and enhance the mechanical properties of the polymer [9]. Most of the researchers recorded the usage of alkaline ion salt to be incorporated in polymer host matrix, such as lithium-ion (Li^+), magnesium-ion (Mg^{2+}), sodium-ion (Na^+) and potassium-ion (K^+) salt [10]. In the past 20 years, the Li^+-based salt system has dominated the development of rechargeable batteries due to its capacity to generate high-performance devices [10-13]. However, because Li^+ salt is expensive and less common on Earth, the use of alternative salts as dopants is being studied.

Pandey *et al.,* [14] stated that magnesium ion (Mg^{2+}) offers a performance capability that is close to that of lithium-ion (Li^+) rechargeable batteries. Magnesium provides numerous advantages, including high atmospheric stability, a high melting point (649 °C), a high energy density (3833 mA·h·cm^{-2}), a slow reaction towards air and water, chemical stability, and a high Earth abundance, which is approximately 104 times higher than Li^+, which is convincing for long-term use [14-16]. Moreover, the speciality of Mg^{2+} salt consists of divalent ions that can exhibit a promising ionic conductivity as it is strongly attracted by the lone pair of oxygen atoms, which promotes salt dissociation and contributes to the transportation of ions [11,17]. The primary reason for the incorporation of magnesium salt polymer matrix is due to the ability of magnesium salt to form a stable ionic bond, which has a small cation size and high lattice energy that results from the strong ion-dipole interaction between the polymer [8,18]. Therefore, magnesium perchlorate ($Mg(ClO_4)_2$) has been chosen as a dopant to be infused in an agarose-based polymer electrolyte.

This research focuses on the incorporation of $Mg(ClO_4)_2$ as a dopant salt in an agarose matrix-based polymer electrolyte to assess its influence on the electrical, structural and electrochemical properties through the characterisations of Electrochemical Impedance Spectroscopy (EIS), Fourier Transform Infrared (FTIR) Spectroscopy, X-ray Diffractometer (XRD) and Linear Sweep Voltammetry (LSV).

2. Methodology

2.1 Materials

The materials used, i.e. polymer agarose (molecular weight, Mw: 630.5 g·mol^{-1}) from Next Gene (Puchong, Malaysia) was used as host polymer, and magnesium perchlorate salt ($Mg(ClO_4)_2$; Mw: 223.20 g·mol^{-1}, ACS reagent 99%) purchased from Sigma-Aldrich (Saint Louis, MI, USA) was used as a dopant salt. The solvent used in this study was Dimethyl sulfoxide (DMSO) with ≥99.7% purity, and 78.129 g·mol^{-1} molecular weight was purchased from Fisher Scientific (Hampton, NH, USA).

2.2 Preparations of Polymer Electrolyte Film

The sample of thin film agarose–$Mg(ClO_4)_2$ polymer electrolyte was prepared by using the solution casting method. 0.5 g of agarose powder was dissolved in 20 ml dimethyl sulfoxide (DMSO) before $Mg(ClO_4)_2$ salt was added to the mixture. The addition of salt varies from 0 to 35 weight percentage (wt%) with a 5 wt% interval. The agarose–DMSO–$Mg(ClO_4)_2$ solution was stirred magnetically until a clear homogeneous solution formed. Then, the solution was cast into a petri dish and dried in an oven until a thin film of agarose–$Mg(ClO_4)_2$ polymer electrolyte sample was observed, as shown in Figure 1. The samples were assigned, as recorded in Table 1, by incorporating various weight percentages of $Mg(ClO_4)_2$ into agarose matrices.

Table 1
The composition of thin film agarose–$Mg(ClO_4)_2$ polymer electrolytes with different amount of salt

Sample Designation	Mass of agarose (g)	Weight percentage of $Mg(ClO_4)_2$ salt (wt%)
0-$Mg(ClO_4)_2$	0.5	0
5-$Mg(ClO_4)_2$	0.5	5
10-$Mg(ClO_4)_2$	0.5	10
15-$Mg(ClO_4)_2$	0.5	15
20-$Mg(ClO_4)_2$	0.5	20
25-$Mg(ClO_4)_2$	0.5	25
30-$Mg(ClO_4)_2$	0.5	30
35-$Mg(ClO_4)_2$	0.5	35

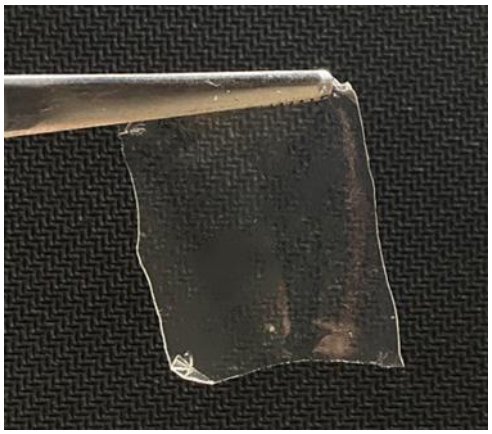

Fig. 1. Example thin film of a selected sample of agarose–$Mg(ClO_4)_2$ polymer electrolyte (30-$Mg(ClO_4)_2$)

2.3 Characterisation Techniques

2.3.1 Electrochemical impedance spectroscopy

Electrochemical impedance spectroscopy (EIS) was performed using a HIOKI 3532-50 LCR Hi-Tester at various temperatures ranging from 300 to 373 K to investigate the electrical properties of polymer electrolytes. The samples were sandwiched between two symmetrical stainless-steel electrodes with a contact area of 0.7854 cm^2. The frequency was fixed during the measurements from 100 Hz to 1 MHz. This measurement measured the parameters related to the ion conduction mechanism, such as ionic conductivity, dielectric and modulus properties.

2.3.2 Fourier transform infrared spectroscopy

The interaction of complex formation in agarose–$Mg(ClO_4)_2$-based polymer electrolyte was analysed by Perkin Elmer FTIR model spectrum 400. The FTIR spectra were obtained in the absorbance mode with a spectral resolution of 2 cm^{-1} in the wave area from 450 to 4000 cm^{-1}. The measurement is taken at room temperature and carried out by an attenuated total reflection (ATR) accessory.

2.3.3 X-ray diffraction spectroscopy

X-ray Diffractometer (XRD) spectroscopy was operated to study the structural characteristics of a polymer film by determining the presence of crystalline or amorphous nature in polymer electrolyte composition. The XRD pattern was performed by PANalytical X'pert PRO diffractometer with CuK_α radiation (λ = 1.5418 Å) and recorded in Bragg angle (2θ) range of 5° to 90° at ambient temperature.

2.3.4 Linear sweep voltammetry

The electrochemical stability of the highest conducting sample of agarose–$Mg(ClO_4)_2$ polymer electrolyte (30–$Mg(ClO_4)_2$) was examined by linear sweep voltammetry (LSV) using an Automatic Battery Cycler (WBCS 3000, WonA Tech, Seoul, South Korea). The sample acts as a separator sandwiched between stainless steel (SS) and magnesium (Mg) metal (Figure 2) at a scan rate of 5 mVs^{-1}. At the same time, the initial and final potential of characterisation is fixed at the range of 0 to 4.0 V. The current curve against voltage was recorded to identify this behaviour by connecting the voltage to the cell.

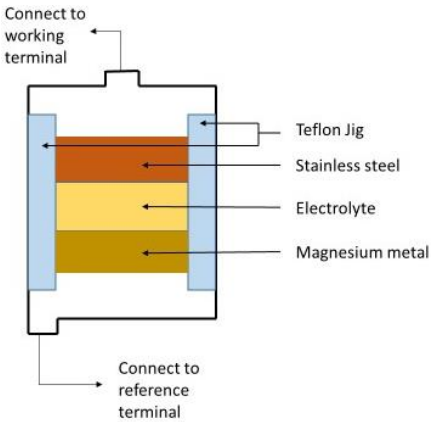

Fig. 2. The configuration used in running LSV's characterisation

3. Results

3.1 Electrical Studies

3.1.1 Ionic conductivity

Ionic conductivity is one of the important parameters related to the electrical properties that need to be determined to ensure the presence of ionic motion in a polymer electrolyte system. This parameter can be analysed by using the formula

$$\sigma = \frac{t}{R_b A} \tag{1}$$

where σ represents the ionic conductivity of the sample ($S \cdot cm^{-1}$), t is the thickness of the thin film (cm), A is the electrode-electrolyte contact area (cm^2), and R_b is the bulk resistance obtained from the intersection of semicircle in high-frequency region and a spike in low-frequency region of impedance plot.

The ionic conductivity of agarose–$Mg(ClO_4)_2$ polymer electrolyte at different weight percentages (wt%) infusion of $Mg(ClO_4)_2$ salt in agarose-based polymer electrolyte is represented in Figure 3. The undoped polymer electrolyte system exhibits a low ionic conductivity value at 1.796×10^{-8} $S \cdot cm^{-1}$ as salt is not added in this system (0 wt%). There is an increment of ionic conductivity to 3.445×10^{-6} $S \cdot cm^{-1}$ after incorporation of 5 wt% of $Mg(ClO_4)_2$ salt and further increase up to 1.222×10^{-5} $S \cdot cm^{-1}$ for sample 15-$Mg(ClO_4)_2$. The ionic conductivity continued to increase significantly and reached its optimum value of ionic conductivity at 6.247×10^{-4} $S \cdot cm^{-1}$ in the composition of 30 wt% $Mg(ClO_4)_2$. The enhancement of ionic conductivity occurs due to the increase in the sample's amorphous nature, which triggers ions' transportation [19]. Moreover, the other factor that affects ionic conductivity is the number of ion dissociations. As seen from the trend of ionic conductivity 0-$Mg(ClO_4)_2$ to 30-$Mg(ClO_4)_2$, the more amount of salt $Mg(ClO_4)_2$ doped in the polymer matrix, the number of ions dissociates into free cation (Mg^{2+}). Free anion (ClO_4^-) increases, thus promoting the ionic conductivity to the optimum ionic conductivity [20]. This result is based on the research conducted by Mahalakshmi *et al.,* [21], where the highest ionic conductivity value was recorded at 4.04×10^{-4} $S \cdot cm^{-1}$ after infusion of 60 wt% $Mg(ClO_4)_2$ in cellulose acetate (CA) polymer.

However, the ionic conductivity decreased to 1.977×10^{-4} $S \cdot cm^{-1}$ when $Mg(ClO_4)_2$ salt was added after the system reached the optimised value. This phenomenon occurs due to the aggregation of ion clusters causing the formation of overcrowded ions, so the free ions are limited to mobile in the matrix [19,21].

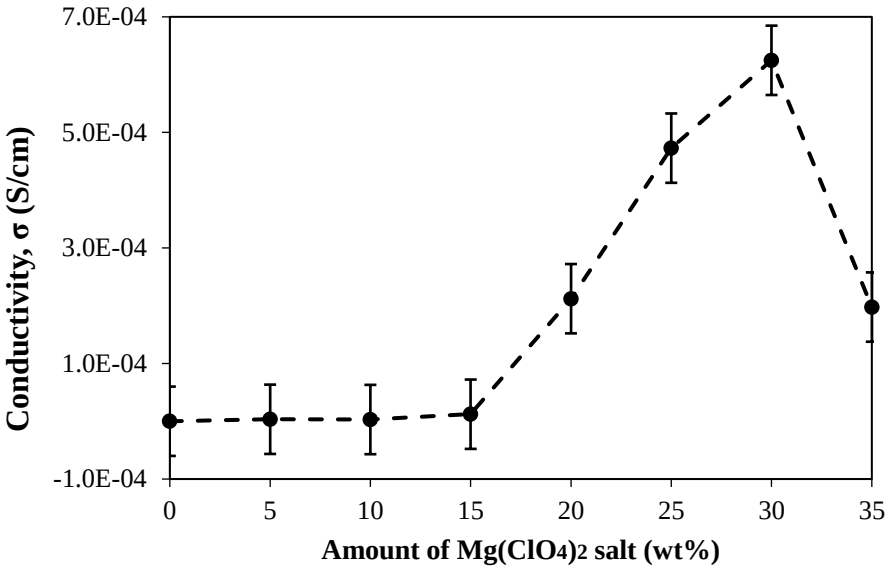

Fig. 3. $Mg(ClO_4)_2$ concentration dependence on DC ionic conductivity at room temperature

3.1.2 Temperature dependence on ionic conductivity studies

Apart from the salt concentration in the polymer matrix, the temperature difference can also influence the ionic conductivity value produced. This correlation is related to the Arrhenius rule, which is denoted as

$$\sigma = \sigma_0 exp^{\frac{-E_a}{k_B T}} \quad (2)$$

where σ_o is the pre-exponential factor, E_a is the activation energy, and k_B is the Boltzmann constant. The relation is proven when the ionic conductivity of agarose–$Mg(ClO_4)_2$ polymer electrolyte is linearly dependent on the temperature and recorded the regression (R^2) value approaching unity as displayed in the graph of log σ against 1000/T (Figure 4). Thus, it has obeyed the Arrhenius rule. The rise in temperature causes the enhancement of ionic conductivity as the supplied thermal energy has weakened ion recombination during the solvent desiccation step of film production and results in more free ions for the conduction process. Therefore, the value of activation energy recorded for the highest conducting sample (30-$Mg(ClO_4)_2$) is the lowest, about 0.105 eV, as displayed in Table 2, which reveals the small energy required for the charge carrier to participate in the conduction process. The samples that have low ionic conductivity, such as 25-$Mg(ClO_4)_2$ and 35-$Mg(ClO_4)_2$, exhibit much higher activation energy (0.123 eV and 0.158 eV, respectively) explained that high energy needed for the free ion to hopping to another coordinating site in agarose–$Mg(ClO_4)_2$ polymer electrolyte [8].

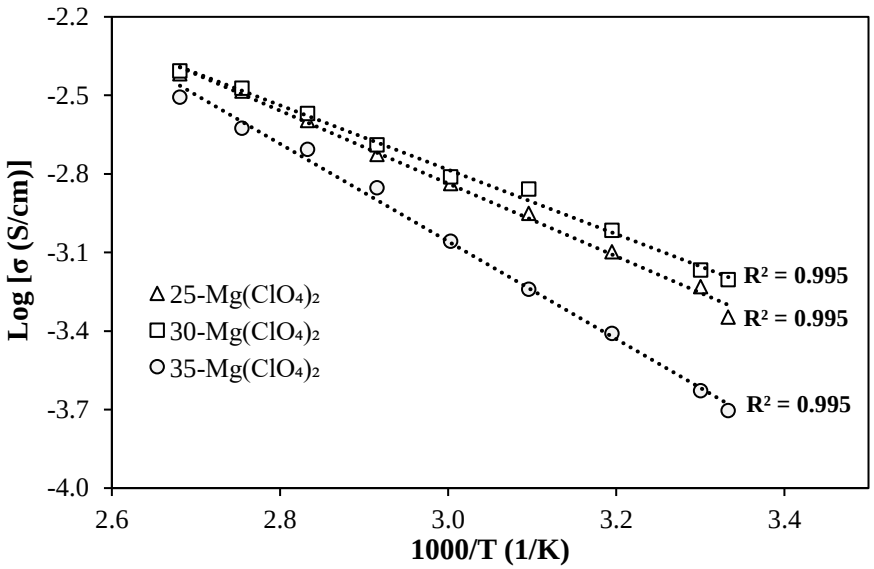

Fig. 4. Temperature-dependent ionic conductivity for the selected samples of agarose-$Mg(ClO_4)_2$ polymer electrolyte system

Table 2
The ionic conductivity and activation energy values of the selected concentration of $Mg(ClO_4)_2$ were incorporated into an agarose matrix

Weight percentage of $Mg(ClO_4)_2$ (wt%)	DC ionic conductivity at 303 K (S·cm^{-1})	DC ionic conductivity at 373 K (S·cm^{-1})	Activation energy, Ea (eV)
25	4.728×10^{-4}	4.015×10^{-3}	0.123
30	6.247×10^{-4}	3.926×10^{-3}	0.105
35	1.987×10^{-4}	3.114×10^{-3}	0.158

3.1.3 Dielectric studies

Dielectric studies were performed to get further information on the conductivity behaviour of the studied divalent ion-based electrolyte. Real and imaginary components of dielectric characteristics define the behaviour of a substance in an electric field. The real component of the dielectric constant, ε_r, quantifies a substance's ability to store electrical charge energy in an electric field. It regulates the amount to which an electric field may penetrate a material and polarise its charges, leading to the build-up of charge on the material's surface, as described by the following equation.

$$\varepsilon_r = \frac{Z_i}{\omega C_0 (Z_r^2 + Z_i^2)} \tag{3}$$

The imaginary component (dielectric loss) measures a material's ability to dissipate electrical energy as heat when subjected to an alternating electric field. It indicates the energy wasted owing to free charges in the material and is proportional to the substance's electrical conductivity:

$$\varepsilon_i = \frac{Z_r}{\omega C_0 (Z_r^2 + Z_i^2)} \tag{4}$$

where, $C_0 = \varepsilon_0 A/t$ and ε_0= the permittivity of free space (8.854×10^{-12} F·m^{-1}). The angular frequency, $\omega = 2\pi f$, Z_r= the real impedance and Z_i = the imaginary impedance. Figure 5 shows the plot of the dielectric constant of the highest conducting sample for agarose–$Mg(ClO_4)_2$ polymer electrolytes system at various temperatures. It illustrates that ε_r decreases gradually as the

frequency rises until the electrode polarisation causes the value to become almost stable at high frequencies. At low frequencies, ε_r increases significantly due to mobile charges migrating along the field before being blocked by blocking electrodes, causing the build-up of ions at the electrode-electrolyte interface to create an electrical double layer [22].

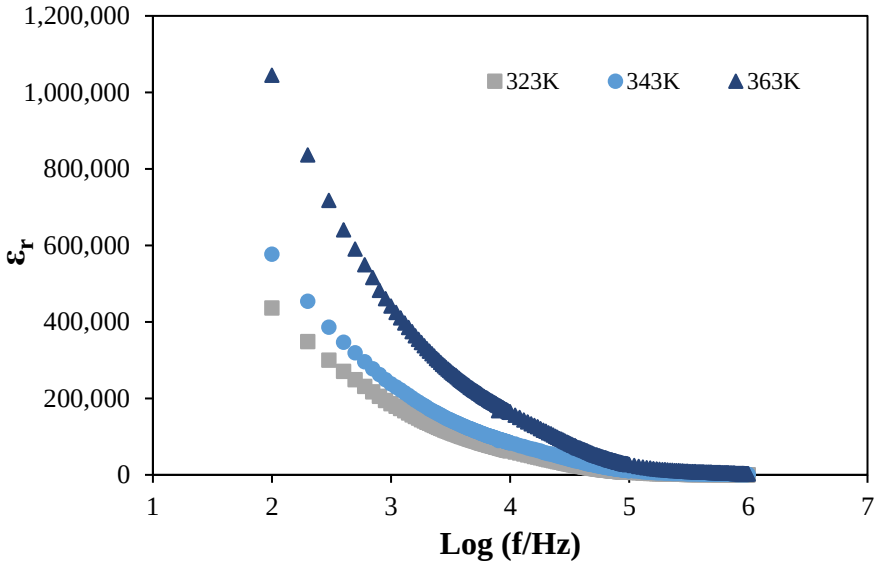

Fig. 5. Variation of the dielectric constant of 30-$Mg(ClO_4)_2$ as a function of frequencies at the selected temperatures

The larger value of the dielectric constant in the low-frequency area is also due to the accumulated charges having enough time to maintain the polarisation. The percentage of free charges that are able to move about increases as the dielectric constant rises. Likewise, as the quantity of free ions rises with temperature, so does the dielectric constant. Since the electric field direction reverses quickly at high frequencies, the dielectric constant value drops and then plateaus in this frequency range, dampening the polarisation effect since no charge can accumulate at the electrode-electrolyte interface. Due to the imprecise polarisation brought on by the random motion of mobile charges, the polarisation effect disappears even at higher temperatures (343 and 363 K) [23].

Dielectric loss, which is related to the amount of energy lost to move ions due to the diffusion and migration process in the system, is illustrated in Figure 6. The figure shows that ε_i has risen more drastic in the low-frequency range as a function of temperature. This finding suggests that more mobile charges are generated, increasing the interaction between randomly moving ions and prolonging the relaxation duration. In the high-frequency range, insufficiencies in charge diffusion and low ε_i values result from the fast reversal of the electric field [23].

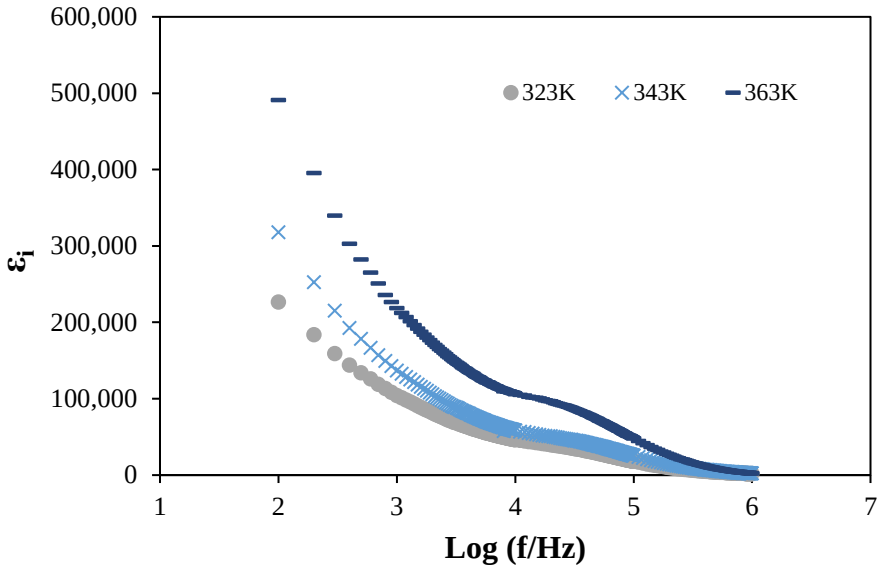

Fig. 6. Variation of dielectric loss of optimised sample of agarose–$Mg(ClO_4)_2$ system as a function of frequencies at selected temperatures

The dielectric analysis is further specified by loss tangent (tan δ) and relaxation time (τ), which is determined by using these relations.

$$\tan \delta = \frac{\varepsilon_i}{\varepsilon_r} \tag{5}$$

$$2\pi f_{max}\tau = 1 \tag{6}$$

The graph of tan δ as a function of the logarithm of frequency (f) for an optimised conducting sample in agarose–$Mg(ClO_4)_2$ polymer electrolytes system at various temperatures is represented in Figure 7. The temperature influences the peak frequency and its intensity in the graphs. Such excitation verified the thermally induced dielectric relaxation process. Materials' ionic charge carriers align with the direction of an applied field, and the longest relaxation time (τ) is attained at higher temperatures. Ions are readily transported and hence participate in conduction and achieve relaxation at a higher frequency, created in high-temperature environments [7]. Table 3 shows the result for this system's highest conducting sample's relaxation time.

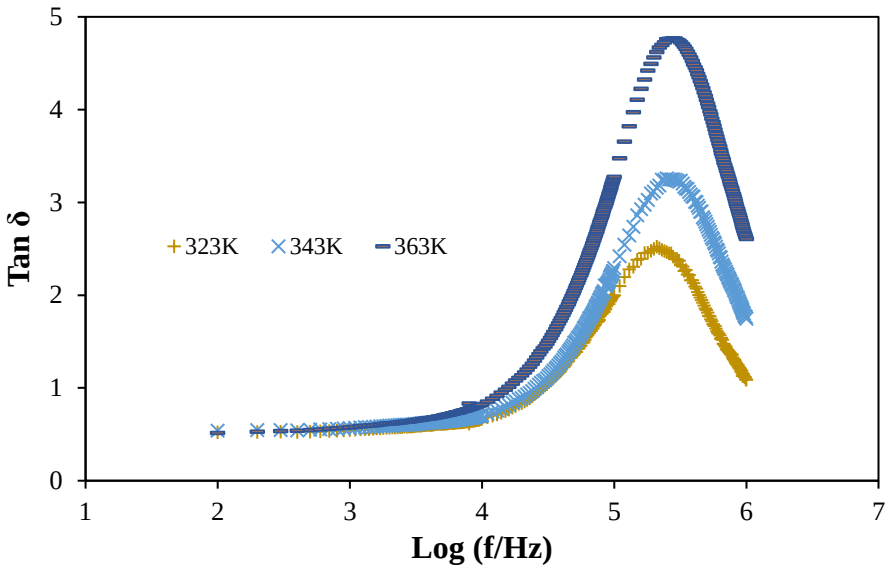

Fig. 7. Graph of tan δ with as a function of the logarithm of frequency for sample 30–$Mg(ClO_4)_2$ system at selected temperatures

Table 3
The value of relaxation time obtained at the selected temperatures for 30 wt% of agarose–$Mg(ClO_4)_2$ sample

Temperature, T (K)	Relaxation time, τ (s)
323	6.9199×10^{-7}
343	5.3052×10^{-7}
363	5.1340×10^{-7}

3.1.4 Modulus studies

The electric modulus formalism has been used to learn more about the behaviour of dielectric materials by lowering the signal intensity associated with electrode polarisation. The dynamical properties of electrical transport processes in materials may be determined, analysed, and interpreted with the help of the complex modulus formalism, which uses variables like the carrier or ion hopping rate and conductivity relaxation time. The electric modulus, M^* is expressed in the complex modulus formula [24]

$$M^* = \frac{1}{\varepsilon_r} = M_r + iM_i \tag{7}$$

where the M_r and M_i are the real part of the modulus and the imaginary part of the modulus that are determined by [25]

$$M_r = \frac{\varepsilon_r}{[(\varepsilon_r)^2+(\varepsilon_i)^2]} \tag{8}$$

$$M_i = \frac{\varepsilon_i}{[(\varepsilon_r)^2+(\varepsilon_i)^2]} \tag{9}$$

where ε_i is the dielectric loss and ε_r is the dielectric constant.

The real part of the modulus (M_r) as functions of frequency for the highest conducting sample at selected temperature are represented in Figure 8, while Figure 9 displays the variation of imaginary electric modulus (M_i) as a function of frequency at the selected temperature for sample 30-$Mg(ClO_4)_2$. A low electric modulus is observed when the electric modulus approaching zero was recorded in the low-frequency regime due to the influence of concealed electrode polarisation effect [23,26]. A long tail at this regime is ascribed to the large capacitance associated with the electrodes, contributing to the non-Debye behaviour in this polymer electrolyte system [25,27]. On the other hand, in the high-frequency regime, both real and imaginary electric modulus increase without clearly identified appearance. The higher values are caused by the bulk effect of the electrolyte samples [28]. In other ways, the temperature rise causes the M_r values to incline, indicating that the charge carriers are moving more quickly.

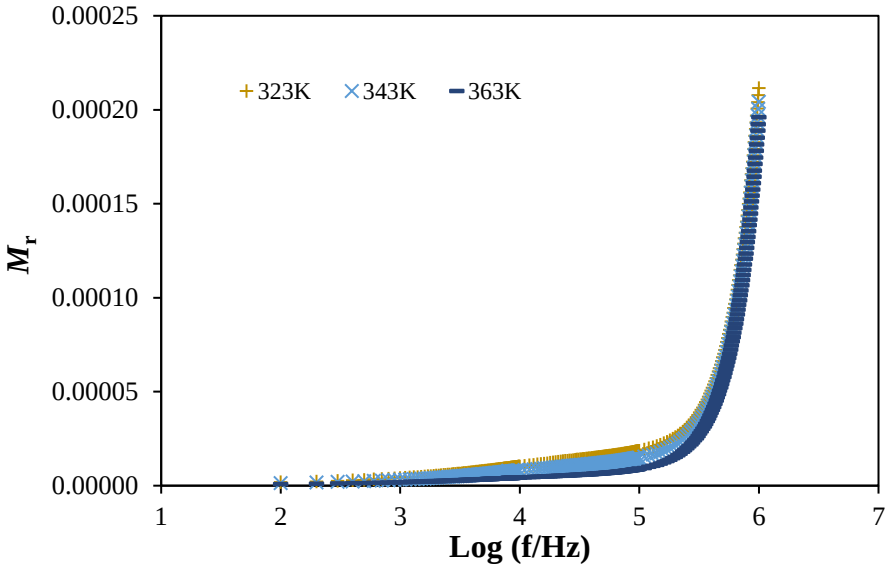

Fig. 8. Variation of the real modulus component for the highest conducting sample of agarose–$Mg(ClO_4)_2$ system as a function of frequencies at the selected temperatures

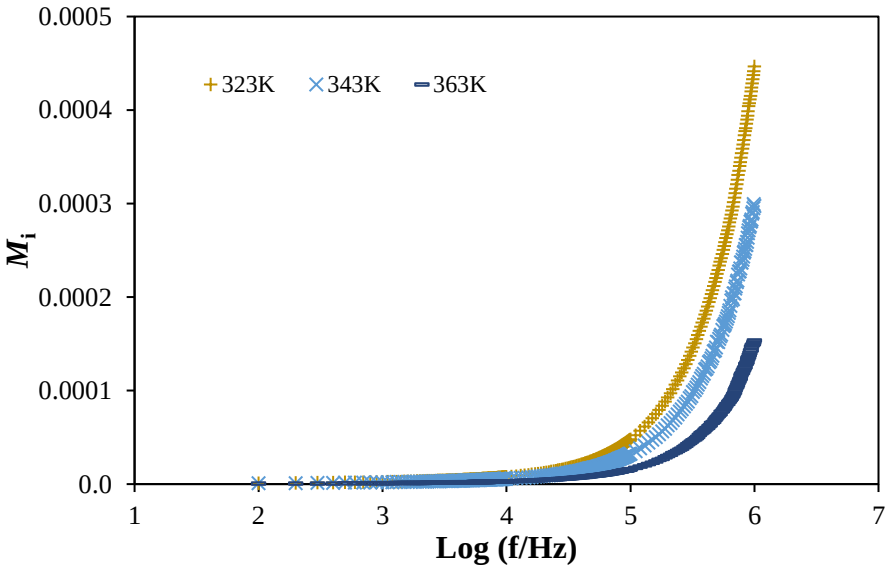

Fig. 9. Variation of the imaginary modulus component for the highest conducting sample of agarose–$Mg(ClO_4)_2$ system as a function of frequencies at the selected temperatures

3.2 Molecular Interaction of Agarose–$Mg(ClO_4)_2$ Polymer Electrolyte

The complexation of agarose with magnesium perchlorate is depicted in FTIR spectra between 450 to 4000 cm^{-1} (Figure 10) and tabulated (Table 4). The first region (i) shows the broad bandwidth of the O-H stretching vibration peak at 3301 cm^{-1} and shifted from 3307 to 3350 cm^{-1} after incorporating salt into the polymer matrix [7,29]. The -CH stretching vibration is observed at 2901 cm^{-1} in 0-$Mg(ClO_4)_2$ [30]. However, after doping the salt, the peak decreased in width and intensity and was recorded the peak at 2920 cm^{-1}. The band at range 1750 cm^{-1}-1650 cm^{-1} shows the stretching vibration of N-H, which centred at 1646 cm^{-1} [7,29]. A medium intensity peak marked at (iv) reveals the appearance of C-C stretching vibration at wavenumber 1436 cm^{-1} [7]. A change of absorption peak at 1366 cm^{-1}-1372 cm^{-1} represents the changes of CH_3 bond bending of agarose after the coordination/complexation of salt with polymer, where the peak was recorded as a drop in intensity. The presence of carbohydrates in this system is testified through the formation of a peak at 1153 cm^{-1}, which belongs to the C-O-C stretching vibration [31]. The peak of the C-OH stretching vibration and the peak of the 3,6-anyhydrogalactose bridge vibration are clearly seen and sustained at 1067 cm^{-1} and 931 cm^{-1}, respectively, regardless of the presence or absence of salt [30,32,33].

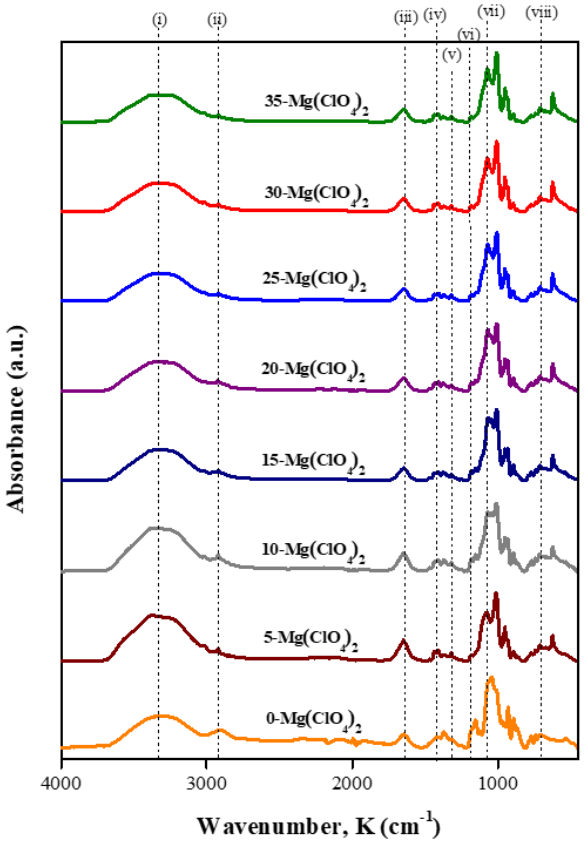

Fig. 10. FTIR spectra of complexation between agarose and $Mg(ClO_4)_2$ in polymer electrolyte system

Table 4
Significant peaks in the FTIR spectrum of agarose–$Mg(ClO_4)_2$ polymer electrolyte

Label	Wavenumber (cm^{-1})	Assignment
i.	3311	*v*(O-H)
ii.	2918	*v*(-CH)
iii.	1647	*v*(N-H)
iv.	1437	*v*(C-C)
v.	1372	*δ*(CH_3)
vi.	1153	*v*(C-O-C)
vii.	1067	*v*(C-OH)
viii.	931	3,6-anyhydrogalactose bridge vibration

v: stretching vibration, *δ*: scissoring (bending)

Further studies related to FTIR are carried out using the FTIR deconvolution technique, which is analysed using the Gaussian function in Origin Lab Software. The region from 600 cm^{-1} to 640 cm^{-1} in the FTIR spectra was selected to create the baseline and then proceeded to be deconvoluted and fitted by the sum of the Gaussian function. The total intensity of all deconvoluted peaks is calculated to validate it had fit the original spectrum and obtained a regression value, R^2 approaching unity (R^2~1) [32]. Figure 11 represents the deconvolution of FTIR spectra for the selected agarose–$Mg(ClO_4)_2$ polymer electrolyte system sample. In this single peak between 600 cm^{-1} to 640 cm^{-1}, there are three peaks observed, which belong to contact/pair ions (green line), free ions (purple line) and ClO_4^- asymmetric bending (blue line). The free ions and contact ions percentages were calculated from the following formulas,

$$Free\ Ion\ (\%) = \frac{A_f}{A_f + A_c} \times 100\% \tag{10}$$

$$Contact\ Ion\ (\%) = \frac{A_c}{A_f + A_c} \times 100\% \tag{11}$$

where A_f is an area under the peak of the free ion region, and A_c is the area under the peak of the contact ion region.

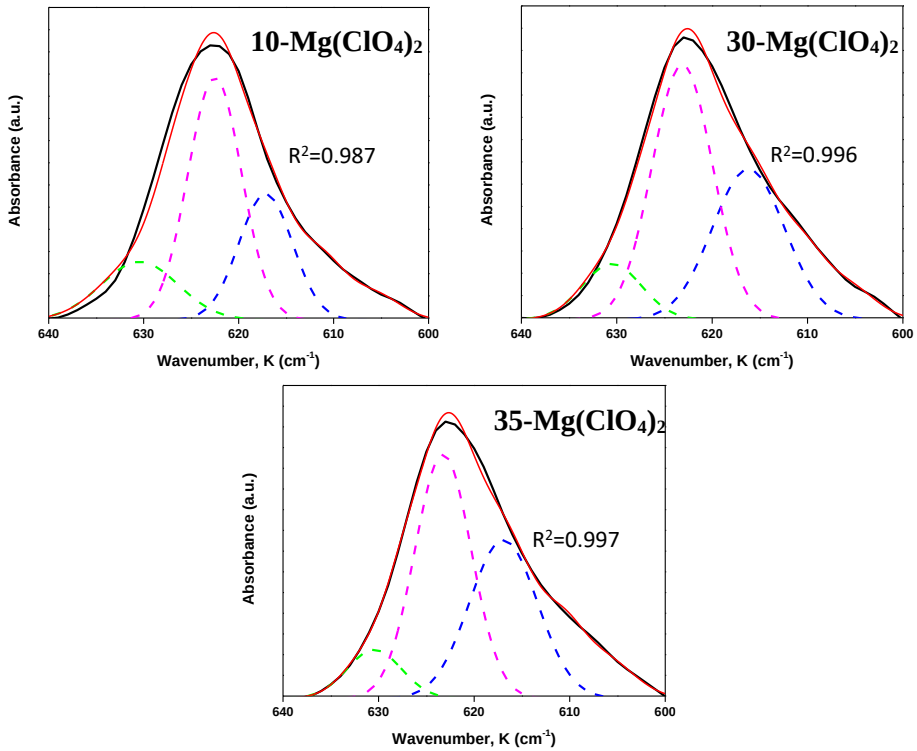

Fig. 11. The possible peaks observed in agarose–$Mg(ClO_4)_2$ polymer electrolyte at wavenumber 600-640 cm^{-1} for selected samples

Due to the electrostatic interaction exerted by the ions' opposing charges in polymer electrolytes, contact ions or ion pairs (Mg^{2+}------ClO_4^-) are detected at the exact wavenumber for all concentrations, which about 630 cm^{-1}, and free ions are most abundant at 623 cm^{-1} [34-36]. This figure demonstrates that the ionic conductivity of a system increases when more salt is doped into its polymer matrix, as the peak area of the contact/pair ions is less than that of the free ions. Figure 12(a) depicts the results of a calculation demonstrating this assertion to be true. The percentage of free ions recorded lowest at 10-$Mg(ClO_4)_2$, which shows the low concentration of free ions associated with small salt addition in the polymer matrix. As the increasing amount of salt was added to the system, the percentage of free ions increased and reached the highest percentage of free ions, about 82% at 30 wt% $Mg(ClO_4)_2$ in accordance with the concentration that obtained the optimum ionic conductivity. The percentage of contact ions contradicts the percentage of free ions, as the lowest percentage of contact ions recorded at 30-$Mg(ClO_4)_2$ proves the mobile ions are favourable at this concentration. However, at 35 wt% addition of $Mg(ClO_4)_2$ in the agarose-based electrolyte, the amount of free ions decreases, but the percentage of contact ions increases due to the aggregation of ions. Therefore, the recorded percentage of free and contact ions was in accordance with the ionic conductivity value obtained in the EIS study, as represented in Figure 12(b). Another additional peak in this range is observed at ~617 cm^{-1}, denoted as ClO_4^- asymmetric band [36].

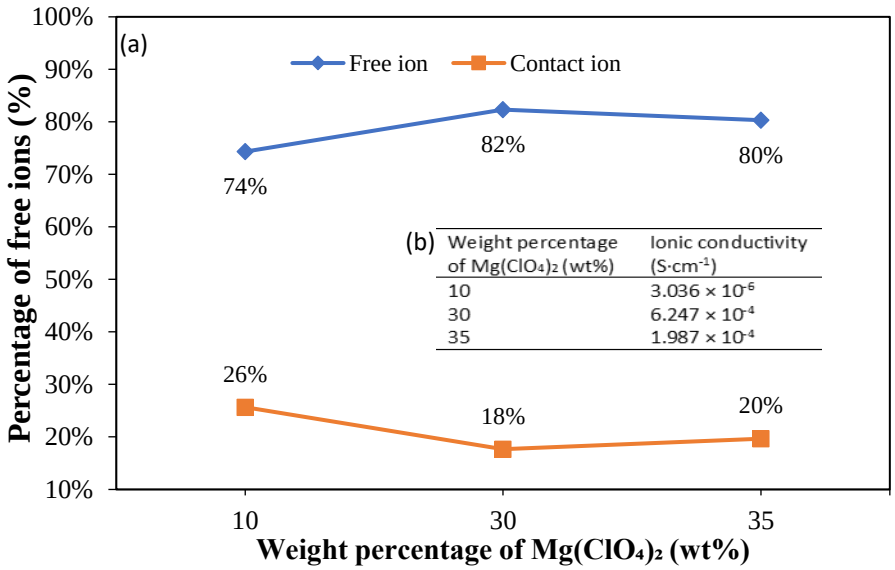

Fig. 12. (a) The percentage of free and contact ions (b) the ionic conductivity recorded in the EIS study for selected samples of agarose–$Mg(ClO_4)_2$ system

3.3 Structural Studies of Agarose–$Mg(ClO_4)_2$ Polymer Electrolyte

Figure 13 shows the samples' XRD pattern of un-doped and doped agarose–$Mg(ClO_4)_2$ complexes. For 0 wt% addition of $Mg(ClO_4)_2$ as the dopant in the agarose polymer matrix, the broad diffraction peaks observed at 19.4° and 22.5° show the semi-crystalline nature of agarose polymer. The peaks have shifted from 15° to 30°, which is recorded in pure agarose powder, which was reported in the study done by Singh *et al.,* [7]. However, the peaks observed in 0-$Mg(ClO_4)_2$ broaden and decrease in intensity with the increasing amount of salt added to the polymer electrolyte system. For 30 wt% incorporation of $Mg(ClO_4)_2$ in agarose-based polymer electrolyte, the two previous peaks have combined and become a single broad peak at 2θ=20° with a decrease in intensity. The change of diffraction peak, which becomes broader and reduces in intensity, indicates the amorphous nature of the electrolyte upon adding salt. Thus, this led to the enhancement of ionic conductivity in the polymer electrolyte system, as stated in the electrical analysis. However, the further addition of $Mg(ClO_4)_2$ salt (35-$Mg(ClO_4)_2$) in the agarose-based polymer electrolyte shows some increment in the intensity of peak due to the failure of the polymer host to accommodate the salt, resulting in ion recombination and a decrease in ionic conductivity [37]. In this XRD pattern, no peak corresponds to the presence of $Mg(ClO_4)_2$ due to the complete dissociation of salt in the polymer matrix, thus enhancing electrical properties.

In order to confirm this result, the structural study has been further by using the deconvolution technique to determine the degree of crystallinity, X_c and the crystallite size, L of agarose–$Mg(ClO_4)_2$ polymer electrolyte film by using formula, respectively

$$X_c = \frac{A_c}{A_c + A_a} \times 100\% \tag{12}$$

where A_c is an area under the peak of the crystalline region and A_a is the area under the peak of the amorphous region,

$$L = \frac{0.9\,\lambda}{FWHM\,\cos\theta} \tag{13}$$

where L is the crystallite size, λ is the X-ray wavelength, fixed at (1.5406Å), FWHM is the full width at half maximum (a measure of the peak broadness), and θ is Bragg's diffraction angle.

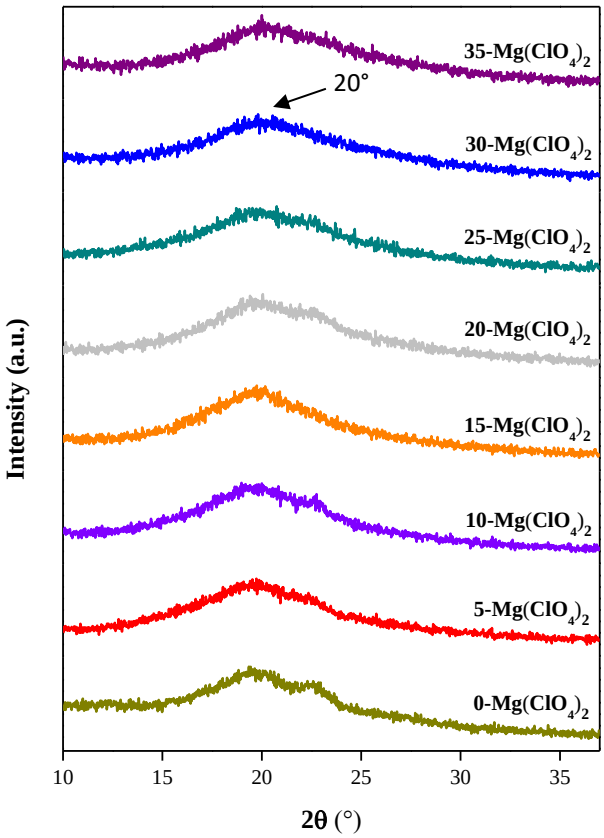

Fig. 13. The XRD pattern of agarose–$Mg(ClO_4)_2$ polymer electrolyte system with different concentration of salt

Figure 14 shows that this system has a semi-crystalline structure, with amorphous (2θ=19-20°; blue peak) and crystalline (2θ=21-24°; green peak) peaks visible after undergoing deconvolution. Crystallite size and degree of crystallinity are determined for each sample by recording the FWHM and the area for each peak after deconvolution (Table 5). The crystallite size shows the decrement from 0 wt% addition of $Mg(ClO_4)_2$ at 6.62 nm to 1.54 nm at 30 wt% addition of salt. The smallest crystallite size recorded at 30-$Mg(ClO_4)_2$ proves the reduction of crystalline nature after the participation of salt in the polymer matrix. At this concentration, the crystalline peak becomes broader and lower in intensity, thus exhibiting the lowest degree of crystallinity, about 27.39%, resulting in the system's highest amorphous nature, promoting the transportation of ions in the polymer matrix [20,38]. Beyond this concentration, the degree of crystallinity is observed to become increase. Mohamed *et al.,* [37] stated that this increment occurred due to salt recrystallisation, which decreased the number density of ions and ionic conductivity. These results have also been supported by the sudden rise in the degree of crystallinity and crystallite size of agarose–$Mg(ClO_4)_2$ polymer electrolyte, which increased to 36.03% and 1.77 nm, respectively. The trend in this structural behaviour also aligns with the findings obtained in electrical and molecular interaction studies, which prove the best amount of salt doped in the polymer matrix is 30 wt% $Mg(ClO_4)_2$.

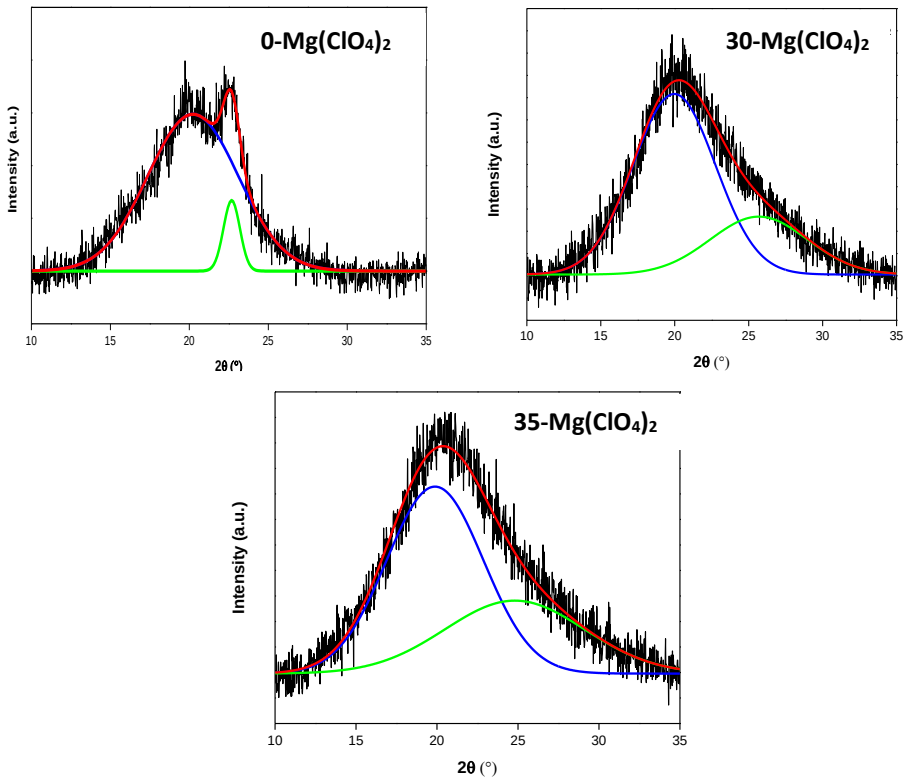

Fig. 14. XRD deconvolution of selected agarose–$Mg(ClO_4)_2$ polymer electrolyte sample

Table 5
The degree of crystallinity, Xc and size of crystallite, L, of selected agarose–$Mg(ClO_4)_2$ polymer electrolyte samples

Samples	Degree of crystallinity, X_c (%)	Crystallite size, L (nm)
0-$Mg(ClO_4)_2$	44.32%	6.62
30-$Mg(ClO_4)_2$	27.39%	1.54
35-$Mg(ClO_4)_2$	36.03%	1.77

3.4 Electrochemical Properties of Agarose–$Mg(ClO_4)_2$ Polymer Electrolyte

Figure 14 portrays the I-V curve generated by LSV for the most conductive agarose–$Mg(ClO_4)_2$ polymer electrolyte system, which is 30–$Mg(ClO_4)_2$. From this curve, the initial current is caused by a redox reaction at the electrode, indicating that mobile species are participating [39]. The current flow was almost constant through the sample until the voltage swept towards the anodic (positive) value and recorded a voltage breakdown at 3.65 V, as denoted in Figure 15, due to the anions' oxidation in the gel polymer electrolyte [40]. The small current value recorded between the cathodic and anodic voltage limit indicates the absence of an electrochemical reaction between the electrode and electrolyte. Thus, the electrochemical potential window stability can be measured from the derivation of cathodic and anodic voltage limits, where the reduction potential of cation (E_{cation}) and oxidation potential of anion (E_{anion}) take place, respectively.

$$Potential\ window = E_{anion} - E_{cation} \tag{14}$$

The voltage breakdown, also known as anodic decomposition limit, indicates the voltage at which current flows through the cells and continues rising rapidly due to electrolyte decomposition at the inert electrode interface [22,39].

The values of cathodic and anodic voltage limits have been labelled as (a) and (b) in Figure 15. Incorporating $Mg(ClO_4)_2$ into the agarose matrix exhibits a wide potential window and higher electrochemical stability up to 3.48 V and 3.65 V, respectively. These values were marked a reasonable range (>3V) for electrochemical applications in magnesium batteries [8,22,41].

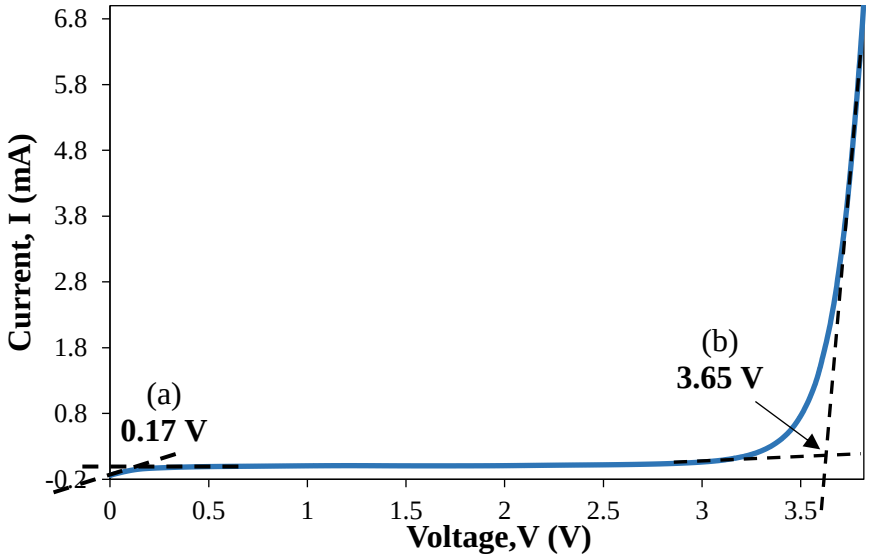

Fig. 15. Graph of LSV curve after incorporating 30 wt% $Mg(ClO_4)_2$ salt into agarose matrix of polymer electrolyte sample

4. Conclusions

Incorporating $Mg(ClO_4)_2$ in agarose-based polymer electrolyte exhibits an optimised ionic conductivity at 6.247×10^{-4} S·cm^{-1} after doping 30 wt% of $Mg(ClO_4)_2$. At this concentration, the value of activation energy required is the lowest, proving the high rate of ion dissociation in this concentration. This system also obeyed the Arrhenius rule, where the ionic conductivity is recorded as increasing with the temperature. In FTIR studies, the presence of peaks observed is the domain found to belong to agarose, which shows the band of ν(O–H), ν(–CH), δ(N–H), $\delta(CH_3)$, ν(C–O–C), ν(C–OH), 3,6–anhydrogalactose bridge vibrations and ν(C–C) in the agarose–based polymer electrolyte. Furthermore, adding $Mg(ClO_4)_2$ reveals the enhancement of its amorphous nature by recording a low degree of crystallinity in XRD analysis. This research is convincing as the complexation between agarose and $Mg(ClO_4)_2$ salt can exhibit wide potential stability and high electrochemical stability polymer electrolyte, which proves that the agarose–$Mg(ClO_4)_2$ polymer electrolyte system has the potential to be employed for an energy storage devices application.

Acknowledgement
The authors appreciatively acknowledge the financial support for this work by the Fundamental Research Grant Scheme (FRGS, Sponsorship File No: FRGS/1/2019/STG07/UITM/02/2; 600-IRMI/FRGS 5/3 (310/2019)), Ministry of Higher Education of Malaysia (MOHE). The authors thank iMADE Research Laboratory, Institute of Science and Faculty of Applied Sciences, UiTM, for supporting this project's research facilities.

References

[1] Singh, Rahul, Pramod K. Singh, Vijay Singh, and B. Bhattacharya. "Agarose biopolymer electrolytes: ion conduction mechanism and dielectric studies." *Cellulose Chemistry and Technology* 51, no. 9-10 (2017): 949-955.

[2] Alves, R., F. Sentanin, R. C. Sabadini, Agnieszka Pawlicka, and Maria Manuela Silva. "Green polymer electrolytes of chitosan doped with erbium triflate." *Journal of Non-Crystalline* Solids 482 (2018): 183-191. https://doi.org/10.1016/j.jnoncrysol.2017.12.038

[3] Varshney, Pradeep K., and Shikha Gupta. "Natural polymer-based electrolytes for electrochemical devices: a review." *Ionics* 17, no. 6 (2011): 479-483. https://doi.org/10.1007/s11581-011-0563-1

[4] Yang, Ying, Hao Hu, Cong-Hua Zhou, Sheng Xu, Bobby Sebo, and Xing-Zhong Zhao. "Novel agarose polymer electrolyte for quasi-solid state dye-sensitized solar cell." *Journal of Power Sources* 196, no. 4 (2011): 2410-2415. https://doi.org/10.1016/j.jpowsour.2010.10.067

[5] Bidikoudi, Maria, Dorothea Perganti, Chaido-Stefania Karagianni, and Polycarpos Falaras. "Solidification of ionic liquid redox electrolytes using agarose biopolymer for highly performing dye-sensitized solar cells." *Electrochimica Acta* 179 (2015): 228-236. https://doi.org/10.1016/j.electacta.2015.02.122

[6] Yang, Ying, Jiarui Cui, Pengfei Yi, Xiaolu Zheng, Xueyi Guo, and Wenyong Wang. "Effects of nanoparticle additives on the properties of agarose polymer electrolytes." *Journal of Power Sources* 248 (2014): 988-993. https://doi.org/10.1016/j.jpowsour.2013.10.016

[7] Singh, Rahul, B. Bhattacharya, S. K. Tomar, Vijay Singh, and Pramod K. Singh. "Electrical, optical and electrophotochemical studies on agarose based biopolymer electrolyte towards dye sensitized solar cell application." *Measurement* 102 (2017): 214-219. https://doi.org/10.1016/j.measurement.2017.02.014

[8] Ali, N. I., Siti Zafirah Zainal Abidin, Siti Rohana Majid, and Nor Kamal Jaafar. "Role of Mg $(NO_3)_2$ as Defective Agent in Ameliorating the Electrical Conductivity, Structural and Electrochemical Properties of Agarose-Based Polymer Electrolytes." *Polymers* 13, no. 19 (2021): 3357. https://doi.org/10.3390/polym13193357

[9] Saari, Riza Asmaa, Muhammad Shahrulnizam Nasri, Takumitsu Kida, and Masayuki Yamaguchi. "Impact of magnesium salt on the mechanical and thermal properties of poly (vinyl alcohol)." *Polymers* 13, no. 21 (2021): 3760. https://doi.org/10.3390/polym13213760

[10] Ramesh, S., Soon-Chien Lu, and Ivo Vankelecom. "BMIMTf ionic liquid-assisted ionic dissociation of MgTf in P (VdF-HFP)-based solid polymer electrolytes." *Journal of Physics and Chemistry of Solids* 74, no. 10 (2013): 1380-1386. https://doi.org/10.1016/j.jpcs.2013.04.017

[11] Aziz, Shujahadeen B., Mohamad A. Brza, Elham M. A. Dannoun, Muhamad H. Hamsan, Jihad M. Hadi, Mohd F. Z. Kadir, and Rebar T. Abdulwahid. "The study of electrical and electrochemical properties of magnesium ion conducting CS: PVA based polymer blend electrolytes: Role of lattice energy of magnesium salts on EDLC performance." *Molecules* 25, no. 19 (2020): 4503. https://doi.org/10.3390/molecules25194503

[12] Gong, Sheng-Dong, Yun Huang, Hai-Jun Cao, Yuan-Hua Lin, Yang Li, Shui-Hua Tang, Ming-Shan Wang, and Xing Li. "A green and environment-friendly gel polymer electrolyte with higher performances based on the natural matrix of lignin." *Journal of Power Sources* 307 (2016): 624-633. https://doi.org/10.1016/j.jpowsour.2016.01.030

[13] Abd Aziz, Mohd Azri, Mohd Saifizi Saidon, Muhammad Izuan Fahmi Romli, Siti Marhainis Othman, Wan Azani Mustafa, Mohd Rizal Manan, and Muhammad Zaid Aihsan. "A Review on BLDC Motor Application in Electric Vehicle (EV) using Battery, Supercapacitor and Hybrid Energy Storage System: Efficiency and Future Prospects." *Journal of Advanced Research in Applied Sciences and Engineering Technology* 30, no. 2 (2023): 41-59. https://doi.org/10.37934/araset.30.2.4159

[14] Pandey, G. P., R. C. Agrawal, and S. A. Hashmi. "Magnesium ion-conducting gel polymer electrolytes dispersed with nanosized magnesium oxide." *Journal of Power Sources* 190, no. 2 (2009): 563-572. https://doi.org/10.1016/j.jpowsour.2009.01.057

[15] Ponraj, T., A. Ramalingam, S. Selvasekarapandian, S. R. Srikumar, and R. Manjuladevi. "Plasticized solid polymer electrolyte based on triblock copolymer poly (vinylidene chloride-co-acrylonitrile-co-methyl methacrylate) for magnesium ion batteries." *Polymer Bulletin* 78, no. 1 (2021): 35-57. https://doi.org/10.1007/s00289-019-03091-5

[16] Sharma, Jyoti, and Safir Hashmi. "Magnesium ion-conducting gel polymer electrolyte nanocomposites: Effect of active and passive nanofillers." *Polymer Composites* 40, no. 4 (2019): 1295-1306. https://doi.org/10.1002/pc.24853

[17] Tang, Xin, Ravi Muchakayala, Shenhua Song, Zhongyi Zhang, and Anji Reddy Polu. "A study of structural, electrical and electrochemical properties of PVdF-HFP gel polymer electrolyte films for magnesium ion battery applications." *Journal of Industrial and Engineering Chemistry* 37 (2016): 67-74. https://doi.org/10.1016/j.jiec.2016.03.001

[18] Guan, Khor Hock, N. K. Farhana, Fatin Saiha Omar, Norshahirah M. Saidi, Shahid Bashir, S. Ramesh, and K. Ramesh. "Influence of tetraglyme towards magnesium salt dissociation in solid polymer electrolyte for electric double layer capacitor." *Journal of Polymer Research* 27 (2020): 1-9. https://doi.org/10.1007/s10965-020-02070-z

[19] Ramlli, M. A., and M. I. N. Isa. "Structural and ionic transport properties of protonic conducting solid biopolymer

electrolytes based on carboxymethyl cellulose doped with ammonium fluoride." *The Journal of Physical Chemistry B* 120, no. 44 (2016): 11567-11573. https://doi.org/10.1021/acs.jpcb.6b06068

[20] Hafiza, M. N., and M. I. N. Isa. "Solid polymer electrolyte production from 2-hydroxyethyl cellulose: Effect of ammonium nitrate composition on its structural properties." *Carbohydrate Polymers* 165 (2017): 123-131. https://doi.org/10.1016/j.carbpol.2017.02.033

[21] Mahalakshmi, M., S. Selvanayagam, S. Selvasekarapandian, V. Moniha, R. Manjuladevi, and P. Sangeetha. "Characterization of biopolymer electrolytes based on cellulose acetate with magnesium perchlorate ($Mg(ClO_4)_2$) for energy storage devices." *Journal of Science: Advanced Materials and Devices* 4, no. 2 (2019): 276-284. https://doi.org/10.1016/j.jsamd.2019.04.006

[22] Manjuladevi, R., M. Thamilselvan, S. Selvasekarapandian, R. Mangalam, M. Premalatha, and S. Monisha. "Mg-ion conducting blend polymer electrolyte based on poly (vinyl alcohol)-poly (acrylonitrile) with magnesium perchlorate." *Solid State Ionics* 308 (2017): 90-100. https://doi.org/10.1016/j.ssi.2017.06.002

[23] Hafiza, M. N., and M. I. N. Isa. "Analyses of ionic conductivity and dielectric behavior of solid polymer electrolyte based 2-hydroxyethyl cellulose doped ammonium nitrate plasticized with ethylene carbonate." In *AIP Conference Proceedings*, vol. 1885, no. 1. AIP Publishing, 2017. https://doi.org/10.1063/1.5002292

[24] Prabu, M., and S. Selvasekarapandian. "Dielectric and modulus studies of $LiNiPO_4$." *Materials Chemistry and Physics* 134, no. 1 (2012): 366-370. https://doi.org/10.1016/j.matchemphys.2012.03.003

[25] Mısenan, Muhammad Syukri Bin, and Azwani Sofia Ahmad Khiar. "Conductivity, dielectric and modulus studies of Methylcellulose-NH4TF polymer electrolyte." *Eurasian Journal of Biological and Chemical Sciences* 1, no. 2 (2018): 59-62.

[26] Hafiza, M. N., A. N. A. Bashirah, N. Y. Bakar, and M. I. N. Isa. "Electrical properties of carboxyl methylcellulose/chitosan dual-blend green polymer doped with ammonium bromide." *International Journal of Polymer Analysis and Characterization* 19, no. 2 (2014): 151-158. https://doi.org/10.1080/1023666X.2014.873562

[27] Khiar, A. S. A., S. R. Majid, N. H. Idris, M. F. Hassan, R. Puteh, and A. K. Arof. "Ionic hopping transport in chitosan-based polymer electrolytes." In *Materials Science Forum*, vol. 517, pp. 237-241. Trans Tech Publications Ltd, 2006. https://doi.org/10.4028/www.scientific.net/MSF.517.237

[28] Fuzlin, A. F., N. A. Bakri, B. Sahraoui, and A. S. Samsudin. "Study on the effect of lithium nitrate in ionic conduction properties based alginate biopolymer electrolytes." *Materials Research Express* 7, no. 1 (2019): 015902. https://doi.org/10.1088/2053-1591/ab57bb

[29] Singh, Rahul, Nitin A. Jadhav, S. Majumder, B. Bhattacharya, and Pramod K. Singh. "Novel biopolymer gel electrolyte for dye-sensitized solar cell application." *Carbohydrate Polymers* 91, no. 2 (2013): 682-685. https://doi.org/10.1016/j.carbpol.2012.08.055

[30] Wang, Weijia, Xueyi Guo, and Ying Yang. "Lithium iodide effect on the electrochemical behavior of agarose based polymer electrolyte for dye-sensitized solar cell." *Electrochimica Acta* 56, no. 21 (2011): 7347-7351. https://doi.org/10.1016/j.electacta.2011.06.032

[31] Shamsuri, Ahmad Adlie, and Rusli Daik. "Utilization of an ionic liquid/urea mixture as a physical coupling agent for agarose/talc composite films." *Materials* 6, no. 2 (2013): 682-698. https://doi.org/10.3390/ma6020682

[32] Hafiza, M. N., and M. I. N. Isa. "Correlation between structural, ion transport and ionic conductivity of plasticized 2-hydroxyethyl cellulose based solid biopolymer electrolyte." *Journal of Membrane Science* 597 (2020): 117176. https://doi.org/10.1016/j.memsci.2019.117176

[33] Tang, Changyu, Ken Hackenberg, Qiang Fu, Pulickel M. Ajayan, and Haleh Ardebili. "High ion conducting polymer nanocomposite electrolytes using hybrid nanofillers." *Nano Letters* 12, no. 3 (2012): 1152-1156. https://doi.org/10.1021/nl202692y

[34] Reddy, M. Jaipal, and Peter P. Chu. "Effect of Mg^{2+} on PEO morphology and conductivity." *Solid State Ionics* 149, no. 1-2 (2002): 115-123. https://doi.org/10.1016/S0167-2738(02)00141-8

[35] Gupta, Ashish, Amrita Jain, and S. K. Tripathi. "Structural and electrochemical studies of bromide derived ionic liquid-based gel polymer electrolyte for energy storage application." *Journal of Energy Storage* 32 (2020): 101723. https://doi.org/10.1016/j.est.2020.101723

[36] Ponmani, S., and M. Ramesh Prabhu. "Development and study of solid polymer electrolytes based on PVdF-HFP/PVAc: Mg $(ClO_4)_2$ for Mg ion batteries." *Journal of Materials Science: Materials in Electronics* 29 (2018): 15086-15096. https://doi.org/10.1007/s10854-018-9649-0

[37] Mohamed, A. S., M. F. Shukur, M. F. Z. Kadir, and Y. M. Yusof. "Ion conduction in chitosan-starch blend based polymer electrolyte with ammonium thiocyanate as charge provider." *Journal of Polymer Research* 27 (2020): 1-14. https://doi.org/10.1007/s10965-020-02084-7

[38] Wang, Bin, Chong Lu, Jing Hu, and Weixin Lu. "Property improvements of EVOH by enhancing the hydrogen bonding." *Plastics, Rubber and Composites* 49, no. 1 (2020): 18-24. https://doi.org/10.1080/14658011.2019.1666465

[39] Ponraj, T., A. Ramalingam, S. Selvasekarapandian, S. R. Srikumar, and R. Manjuladevi. "Mg-ion conducting triblock copolymer electrolyte based on poly (VdCl-co-AN-co-MMA) with magnesium nitrate." *Ionics* 26, no. 2 (2020): 789-800. https://doi.org/10.1007/s11581-019-03244-6

[40] Syahidah, S. Nuur, and S. R. Majid. "Ionic liquid-based polymer gel electrolytes for symmetrical solid-state electrical double layer capacitor operated at different operating voltages." *Electrochimica Acta* 175 (2015): 184-192. https://doi.org/10.1016/j.electacta.2015.02.215

[41] Xu, Kang, Michael S. Ding, and T. Richard Jow. "A better quantification of electrochemical stability limits for electrolytes in double layer capacitors." *Electrochimica Acta* 46, no. 12 (2001): 1823-1827. https://doi.org/10.1016/S0013-4686(01)00358-9